

# Microstructure and Multifaceted Properties of Al-Si-Mg Alloys

Dr. Sofia Jensen, Prof. Liam Chen

Massachusetts Institute of Technology, Cambridge, USA

**Abstract**—In recent years, the use of the aluminum based alloys in the industry and technology are increasing. Alloying elements in aluminum have further been improving the strength and stiffness properties that provide superior compared to other metals. In this study, investigation of physical properties (microstructure, microhardness, tensile strength, electrical conductivity and thermal properties) in the Al-12.6wt.%Si-2wt.%Ni ternary alloy were investigated. Al-Si-Ni alloy was prepared in vacuum atmosphere. The samples were directionally solidified upwards with different growth rate  $V$  (8.3–165.45  $\mu\text{m/s}$ ) at constant temperature gradient  $G$  (7.73 K/mm). The flake spacings ( $\lambda$ ), microhardness (HV), ultimate tensile strength ( $\sigma$ ), electrical resistivity ( $\rho$ ) and thermal properties ( $\Delta H$ ,  $C_p$ ,  $T_m$ ) of the samples were measured. Influence of the growth rate and spacings on microhardness, ultimate tensile strength and electrical resistivity were investigated and relationships between them were obtained. According to results,  $\lambda$  values decrease with increasing  $V$ , but  $HV$ ,  $\sigma$  and  $\rho$  values increase with increasing  $V$ . Variations of electrical resistivity ( $\rho$ ) of solidified samples were also measured. The enthalpy of fusion ( $\Delta H$ ) and specific heat ( $C_p$ ) for the alloy was also determined by differential scanning calorimeter (DSC) from heating trace during the transformation from liquid to solid. The results in this work were compared with the previous similar experimental results.

**Keywords**—Electrical resistivity, enthalpy, microhardness, solidification, tensile stress.

## I. INTRODUCTION

**D**IRECTIONAL solidification enables formation of materials during transition from liquid to solid state along direction specified through thermal gradient and growth rate [1]. As first directional solidification was applied to prepare turbine blades, and can be used to improve functional and structural characteristics of materials, such as single crystal super alloys, high temperature intermetallic compounds, in situ eutectic composites. Directional solidification technique is also an important research instrument to study solidification theory of metals and alloys, because it helps to achieve controllable cooling rate in a broad range, solidification structure from near-equilibrium to far-from equilibrium, interface evolution, solute redistribution, phase selection, crystal growth instability [2]–[4]. From directional solidification well known are instruments of Czochralski, Bridgman-Stockbarger and Chalmers [5], [6].

The automotive and aircraft industrial needs led to increasing application of Al-Si based alloys thanks to the great potential of these materials as replacements for heavier materials (steel, cast

iron or copper) [7], [8]. The Al-Si alloy system, which is characterized by high specific strength, excellent corrosion resistance, as well as good thermal and electrical conductivities, is widely used to supplant other alloys in the areas of transportation, packaging, construction, and machinery to achieve great weight reduction [9].

It is known that the mechanical and electrical properties of metallic materials are affected by their morphology. The mechanical and electrical properties of directional solidified Al-base alloys which are important commercial materials have been reported in several investigations [10], [11] but the results differ from each other. The microstructure evolution during solidification depends on the alloy characteristics and primarily is a function of the temperature profiles at the solidification interface. When a eutectic or near-eutectic alloy is solidified, the most frequently observed solid morphology is regular or irregular lamellar eutectic microstructures [12]. Microstructures are characterized by the microstructure parameters. Numerous solidification studies have been reported with a view to characterizing the microstructure parameters as a function of growth rate ( $V$ ) [13], [14].

The aim of the present work was to experimentally investigate the dependency of the flake spacing ( $\lambda$ ) on growth rate and investigate the mechanical, electrical and thermal properties of the directionally solidified Al-Si-Ni ternary alloy.

## II. EXPERIMENTAL PROCEDURE

### A. Sample Preparation and Solidification

In this work, Al-12.6wt. %Si-2wt. %Ni ternary alloy was prepared in a vacuum atmosphere by using aluminum, silver and nickel of purity of 99.99%. After allowing time for melt homogenization, the molten alloy was poured into 10 graphite (250 mm in length, 4 mm ID and 6.35 mm OD) held in a specially constructed hot filling furnace at about 50 K above the melting point of the alloy. The molten metal was then directionally solidified from bottom to top to ensure that the crucible was completely full. Then, each sample was positioned in a Bridgman type furnace in a graphite cylinder (300 mm in length 10mm ID and 40 mm OD). In this technique, the sample was heated about 200 K above the melting temperature and the sample was then growth by pulling it downwards by synchronous motors. After 10-12 cm steady state growth, the samples were quenched by rapidly pulling it down into the water reservoir. The melting point of Al-Si-Ni ternary alloy is about 856.68 K. The temperature of water in the reservoir was kept at 278 K with accuracy of  $\pm 0.1$  K by using a digital heating / refrigerating circulating bath (model 9102; Poly Science). The sample temperature was also controlled to accuracy of  $\pm 0.1$  K using a Eurotherm 2604 type controller. Solidification of the samples was carried with different growth rates ( $V=8.32-165.45 \mu\text{m/s}$ ) at a constant  $G$  (7.73 K/mm).

*B. Measurement of Growth Rate and Temperature Gradient*

Three temperatures in the samples were measured by Ktype thermocouples which were fixed within the sample with spacing of 10-20 mm. All the thermocouple's ends were then connected the measurement unit consists of data-logger and computer. The cooling rates were recorded with a data-logger via computer during the growth. When the solid/liquid interface was at the second thermocouple, the temperature difference between the first and second thermocouples ( $\Delta T$ ) was read from data-logger record. The time taken for the solid-liquid interface phases the thermocouples separated by known distances was read from data-logger record. Thus, the value of growth rate ( $V = \Delta X / \Delta t$ ) for each sample was determined using the measured value of  $\Delta t$  and known value of  $\Delta X$ . The temperature gradient ( $G = \Delta T / \Delta X$ ) in the liquid phase for each sample was determined using the measured values of  $\Delta T$  and  $\Delta X$ .

*C. Metallographic Examination*

The quenched samples were removed from the graphite crucible and 3 cm in lengths from the top and bottom were cropped off and discarded. Then the rest of the samples ground to observe the solid-liquid interface and the longitudinal section, which included the quenched interface was separated from the specimen. These parts of specimens were mounted in a cold-setting epoxy-resin. The longitudinal and transverse sections were wet-ground down to 2500 grit and mechanically polished using 6- $\mu\text{m}$ , 3- $\mu\text{m}$ , 1- $\mu\text{m}$ , and 0.25 $\mu\text{m}$  diamond paste. Finally the samples were etched with an acid solution (5 ml hydrofluoric acid, 95 ml distilled water) to reveal the microstructure. The microstructures of samples were characterized from both transverse and longitudinal sections of samples using LEO scanning electron microscopy (SEM) (see Figs. 1 and 2).

*D. The Measurement of Microhardness and Tensile Stress*

One of the purposes of this investigation was to obtain the relationships among growth rate, flake spacing, microhardness and tensile stress. The mechanical properties of any solidified materials are usually determined with hardness test, tensile stress test, compressive stress test, ductility test, etc. Since true tensile stress testing of solidified alloys gave inconsistent results with a wide scatter due to the strong dependence on the solidified sample surface quality, the mechanical properties were monitored by hardness testing, which is one of the easiest and most straightforward techniques.

The Vickers hardness (HV) is the ratio of a load applied to the indenter to the surface area of the indentation. This is given by

$$HV = 2P \sin(\theta/2) \tag{1}$$

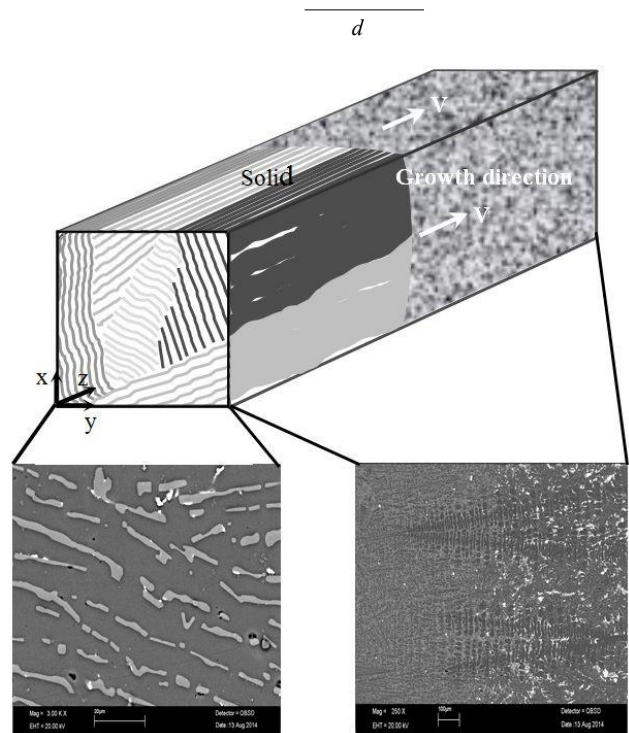


Fig. 1 Schematic illustration of the growth direction and microstructure on longitudinal and transverse sections

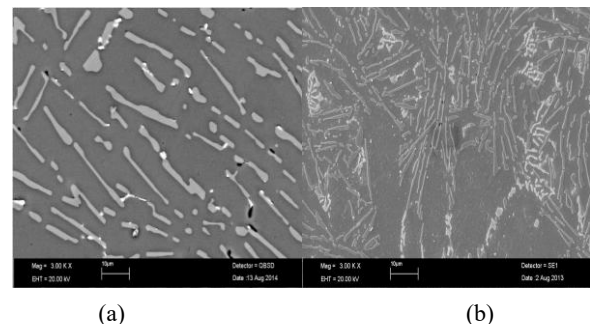


Fig. 2 Typical images of the growth morphologies of directionally solidified Al-Si-Ni alloy at a constant G (7.73 K/mm) (a)  $V=8.32\mu\text{m/s}$  (b)  $V=165.45\mu\text{m/s}$

Microhardness measurements in present work were made with a *DuraScan* model hardness measuring test device using a (10-50 g) load and a dwell time of 10 s giving a typical indentation depth about 40-60  $\mu\text{m}$ , which is significantly smaller than the original solidified samples. The minimum impression spacing (center to edge of adjacent impression) was about 3 times the diagonal and was located at least 0.5 mm from the edge of sample. The microhardness was the average of at least 30 measurements on the sample.

The tests of tensile stresses was performed at room temperature with a *Shimadzu AG-IS universal testing machine*.

The data collected from the tensile test can be analysis using the following formula to determine the stress ( $\sigma$ );

$$\sigma = \frac{F}{A} \quad (2)$$

where,  $\sigma$  is the stress in  $\text{N/mm}^2$  (or MPa),  $F$  is the applied force (N),  $A$  is the original cross sectional area of the sample. The measurements of tensile strength were made at room temperature at a strain rate of  $10^{-3} \text{ s}^{-1}$  with a *Shimadzu AG-XD universal testing machine*. The round rod tensile and compressive samples with diameter of 4 mm and gauge length of 15 mm were prepared from directionally solidified rod samples with different growth rates ( $V=8.32\text{-}165.45 \text{ }\mu\text{m/s}$ ) at a constant  $G$  (7.73 K/mm).

#### E. Measurement of Electrical Resistivity

Another purpose of this investigation was to obtain the relationships among the solidification parameters, microstructures and electrical resistivity. The electrical resistivity of directionally solidified samples was measured by the d.c. four-point probe method [6]. The four-point probe method is the most widely used technique for electrical profile measurement of materials.

In this method, the material's resistivity can be expressed as,

$$\rho = RCF \frac{V}{I} \quad (3)$$

where, RCF is resistivity correction factor,  $V$  is the potential difference measured across the probes and  $I$  is the current through the probes. The geometry of the sample determines the correction factors that must be used, additionally the position of the probes on the sample and the spacing between the probes. The need for correction factors is caused by the proximity of a boundary which limits the possible current paths in the sample. The number of RCF is calculated by diameter of sample divided by probe spacing (probe spacing being the distance between any two adjacent probes). In this study, a 4mm diameter sample probed with a four point probe with 1mm tip spacing would have a correction factor of 0.65.

When a constant current was applied on the sample with a *Keithley 2400* source meter the potential drops on the samples were measured with a *Keithley 2700* multimeter connected to a computer. Platinum wire, 0.5 mm in diameter was used to be the probes of current and potential.

Two of the probes are used to source current and the other two probes are used to measure voltage, using four probes eliminates measurement errors due to the probe resistance, the spreading resistance under each probe, and the contact resistance between each metal probe and material, [15]. The sizes of samples were measured by using a digital micrometer, has an accuracy of 1  $\mu\text{m}$ . The error in the electrical resistivity measurements is calculated about 5%. This error is due to current, voltage and temperature measurements.

#### F. Determination of Enthalpy and Specific Heat

The enthalpy of fusion ( $\Delta H$ ) and the specific heat ( $C_p$ ) of the ternary eutectic alloy (~10 mg) were determined because they are very important parameters for industrial applications. DSC

thermal analysis (Perkin Elmer Diamond model) was performed in the temperature from 400 K to 1200 K at a heating rate of 10 K/min under a constant stream of nitrogen at atmospheric pressure. We used a reference material (a sapphire disk) in determining specific heat change. This reference data is used to "correct" sample data at every temperature. The size of the signal which is used to calculate the specific heat change is proportional to the heating rate, so it follows that faster heating rates will produce larger signals, which would give more accurate data. However, if the heating rate is too high, the temperature gradients in the sample will be large and this may introduce other errors in the measurement. It is normal to use heating rates between 5 K/min and 20 K/min. The heating rate in this study was 10 K/min, which is mostly recommended.

The difference between the sample curve and the baseline curve is measured in mill watts and converted to specific heat change as,

$$C_p = \frac{dQ}{m\beta} \quad (4)$$

where  $dQ/dt$  is heat flow,  $m$  is the mass of the sample, and  $\beta$  is the heating rate in K/min.

### III. RESULTS

#### A. Effect of Growth Rate on Flake Spacing

Variations of eutectic spacing ( $\lambda$ ) with the growth rate ( $V$ ) at a constant  $G$  (7.73 K/mm) is given in Fig. 3 and Table I. The variation of  $\lambda$  versus  $V$  can be given the proportionality equation as,

$$\lambda = k_1 V^a \quad (5)$$

where  $k_1$  is constant and  $a$  is an exponent value of growth rate. The relationships between the flakes spacing and growth rates were determined as  $\lambda = 21.5 V^{-0.43}$  by using linear regression analysis. The exponent value 0.43 is in good agreement with the range values of 0.39-0.46 obtained by different researchers [10]-[14].

#### B. The Effect of Growth Rate on Microhardness

As mentioned above, Al-Si-Ni bulk samples were directionally solidified under constant temperature gradient ( $G=7.73 \text{ K/mm}$ ) with different growth rates ( $V=8.32\text{-}165.45 \text{ }\mu\text{m/s}$ ). It can be seen from Table I that an increase in the temperature gradient and growth rate leads to an increase in the microhardness. Dependence of the HV on the  $V$  and  $\lambda$  were determined by using linear regression analysis and the relationship between them can be expressed by,

$$HV = k_2 V^b \quad (6)$$

$$HV = k_3 \lambda^c \quad (7)$$

increased with

4, ultimate tensile strength (UTS,  $\sigma$ ) values are

where  $k_2$  and  $k_3$  are constant,  $b$  and  $c$  are the exponent values of the growth rate and flake spacing, respectively. As can be seen from Figs. 4 and 5, the microhardness values increase with the increasing  $V$  values and decreasing with the increasing  $\lambda$  values. It is found that increasing growth rate from  $8.32 \mu\text{m/s}$  to  $165.45 \mu\text{m/s}$ , microhardness increases from  $66.25 \text{ kg/mm}^2$  to  $83.03 \text{ kg/mm}^2$  and also decreasing flake spacing from  $8.26 \mu\text{m}$  to  $2.72 \mu\text{m}$ , microhardness increases. The average exponent values of  $V$  and  $\lambda$  for HV in the directionally solidified Al-Si-Ni alloy were found to be 0.07 and 0.16, respectively in this work. These exponent values relating to  $V$  and  $\lambda$  obtained in present work is generally in a good agreement with the exponent values obtained

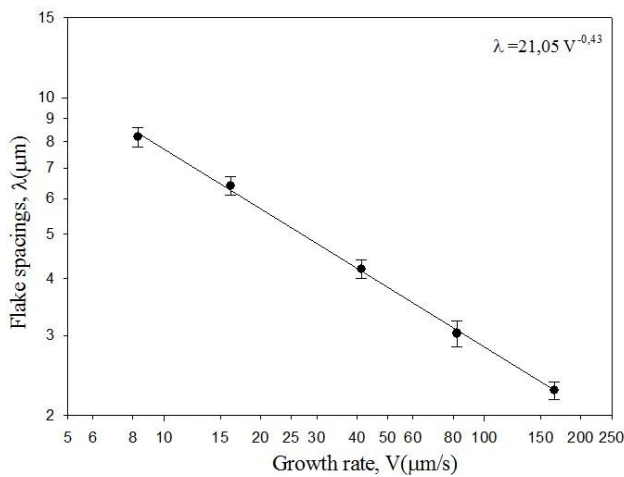


Fig. 3 Variation of flakes spacing as a function growth rate

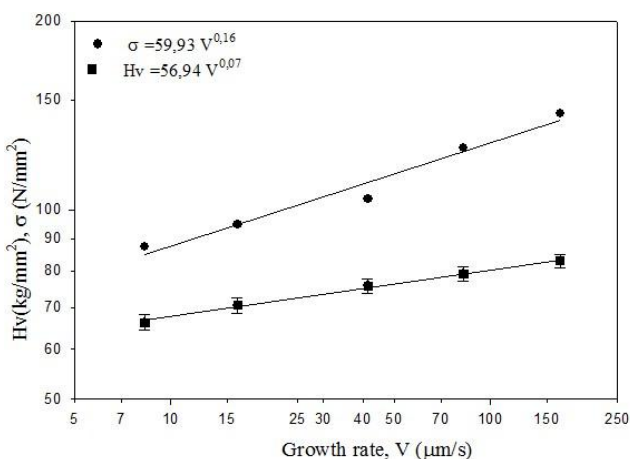


Fig. 4 Variation of microhardness, Hv, and tensile strength  $\sigma$  as a function growth rate

### C. The Effect of the Growth Rate on Ultimate Tensile Strength

Typical strength-strain curves of Al-Si-Ni alloy are shown in Figs. 4 and 5 for  $V$  and  $\lambda$  values. As can be seen from Fig. increasing  $V$ , but flake spacing values are increased ultimate tensile strength decreased.

Figs. 4 and 5 shows the variation of the  $\sigma$  with the  $V$  and  $\lambda$ . The dependence of  $\sigma$  on  $V$  and  $\lambda$ , can be represented as,

$$\sigma = k_4 V^d \quad (8)$$

$$\sigma = k_5 \lambda^e \quad (9)$$

As can be seen from Figs. 4 and 5 and Table I, the values of  $\sigma$  increase with increasing  $V$ . It was found that increasing  $V$  from  $8.32 \mu\text{m/s}$  to  $165.45 \mu\text{m/s}$ , the UTS values increase from  $87.40 \text{ MPa}$  to  $142.70 \text{ MPa}$ . The exponent value of  $V$  is found to be 0.16. And also, it was found that decreasing  $\lambda$  values from  $8.26 \mu\text{m}$  to  $2.72 \mu\text{m}$ , the UTS values increase from  $87.40 \text{ MPa}$  to  $142.70 \text{ MPa}$ . The exponent value of  $\lambda$  is found to be 0.37 (Fig. 5).

in previous experimental works [16]-[19] under similar solidification conditions.

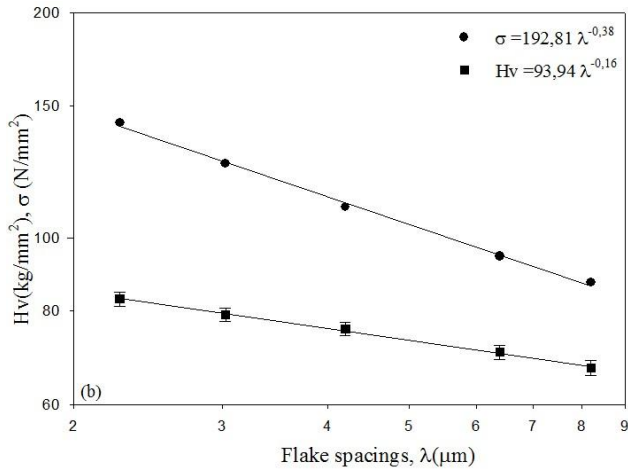


Fig. 5 Variation of microhardness,  $H_v$ , and tensile strength  $\sigma$ , as function flake spacings

#### D. Dependence of the Electrical Resistivity on the Growth Rate and Flake Spacings

It can be seen from Table I, the temperature gradient and growth rate lead to an increase in the electrical resistivity. The dependence of the electrical resistivity on the growth rate and flake spacings can be expressed as

$$\rho = k_6 V^f \quad (10)$$

$$\rho = k_7 \lambda^g \quad (11)$$

where  $k_6$  and  $k_7$  are constants which can be experimentally determined and given in Table I. The value of the exponent relating to the growth rate and flake spacings was obtained to be 0.05 and 0.14, respectively (Figs. 6 and 7). Such a tendency is quite natural result. Because the changes of resistivity of pure metals and alloys depending on microstructure evolution. Change of resistivity can be interpreted as indicating that some other mechanism, such as electron–electron interaction, grain boundary/impurity scattering, etc., is involved in the electrical conduction process [20]. The similar trend is supported by [21].

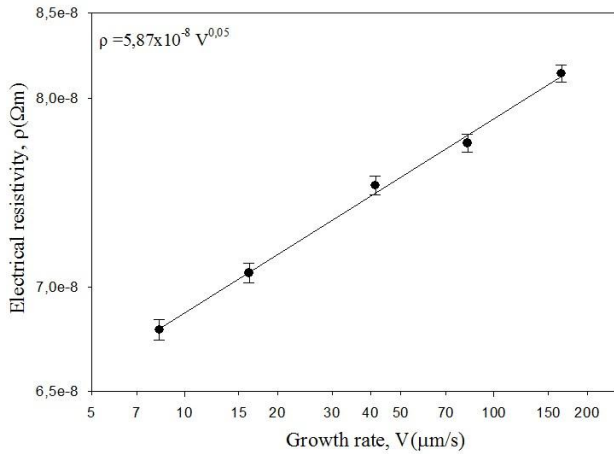


Fig. 6 Variation of electrical resistivity as a function growth rate

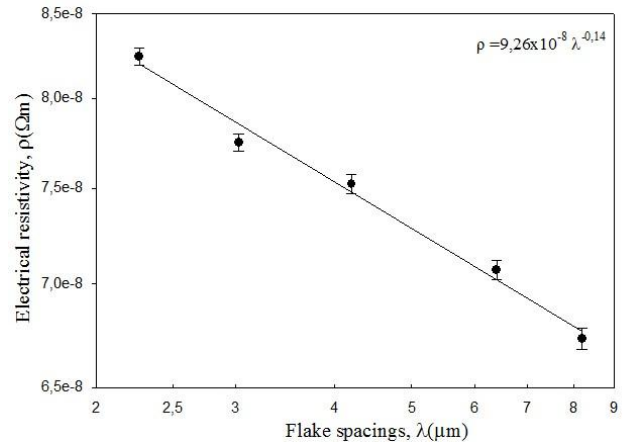


Fig. 7 Variation of electrical resistivity as a function flake spacings

### E. The Thermal Properties of Al-Si-Ni Alloy

The Al-Si-Ni alloy was heated with a heating rate of 10 K/min from room temperature to 1200 K by using a *Perkin Elmer Diamond* model DSC and the heat flow versus temperature is given in Fig. 8. As can be seen from Fig. 8, the melting temperature of Al-Si-Ni alloy was found to be 856.68 K. The values of the enthalpy of fusion and the specific heat were also calculated to be 209.31 J/g and 0.244 J/(g.K) respectively from the graph of the heat flow vs. temperature. The recommended values of the enthalpy of fusion for pure Al, Si, Ni and Al-Si eutectic are 396.96 J/g, 111 J/g, 297.83 J/g and 468.2 J/g respectively, and also, the specific heat values for pure Al, Si, Ni and Al-Si eutectic are 0.897 J/gK, 0.230 J/gK, 0.444 and 0.563 J/gK, in respectively [19], [20] at the melting temperature. The ΔH (209.31 J/g) and Cp values (0.244J/gK) are smaller than the values of pure Al, Ni and AlSi eutectic (Fig. 8).

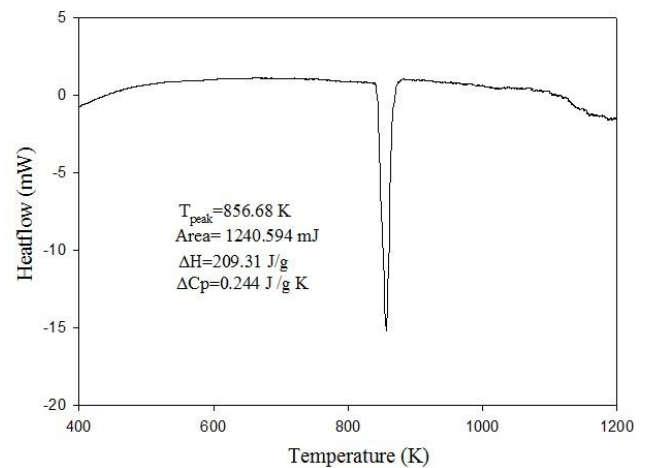


Fig. 8 Heat flow versus temperature for Al-Si-Ni alloy at heating rate of 10 K/min

REFERENCES

[1] Fraś, E. (2003), Solidification of Metals. Warszawa: Wydawnictwo

TABLE I  
EXPERIMENTAL RESULTS AND RELATIONSHIPS FOR DIRECTIONAL SOLIDIFIED AL-12.6WT%SI-2WT%NI TERNARY ALLOY

Solidification parameters		Microstructures, microhardness and electrical resistivity			
<i>V</i> (μm/s)	<i>G</i> (K/mm)	$\lambda$ (μm)	$\sigma$ (MPa)	<i>HV</i> (kg/mm <sup>2</sup> )	$\rho \times 10^{-8}(\Omega \text{ m})$
8.32	7.73 (constant)	8.260	87.40	66.25	6.79
16.27		6.460	94.70	70.55	7.07
41.43		4.250	104.10	75.71	7.52
82.35		3.070	125.80	79.10	7.75
165.45		2.720	142.70	83.03	8.14
Relationships		Constant (k)	Correlation coefficients (r)		
$\lambda = k_1 V^{-0.43}$		$k_1 = 21.05 (\mu\text{m}^{1.43} \text{s}^{-0.43})$	$r_1 = 0.999$		
$HV = k_2 V^{0.07}$		$k_2 = 95.36 (\text{kg mm}^{-2.07} \text{s}^{0.07})$	$r_2 = 0.997$		
$HV = k_3 \lambda^{-0.16}$		$k_3 = 31.01 (\text{kg mm}^{-1.84})$	$r_3 = 0.998$		
$\sigma = k_4 V^{0.16}$		$k_4 = 187.49 (\text{MPa mm}^{-0.16} \text{s}^{0.16})$	$r_4 = 0.983$		
$\sigma = k_5 \lambda^{-0.37}$		$k_5 = 13.82 (\text{MPa mm}^{0.37})$	$r_5 = 0.986$		
$\rho = k_6 V^{0.05}$		$k_6 = 9.21 (\Omega \mu\text{m}^{0.95} \text{s}^{0.05})$	$r_6 = 0.998$		
$\rho = k_7 \lambda^{-0.14}$		$k_7 = 3.30 (\Omega \mu\text{m}^{1.14})$	$r_7 = 0.993$		

$\lambda$ : The average values of flake spacings measured from transverse section, *HV*: The average values of the microhardness measured from the longitudinal and transverse sections,  $\sigma$ : The values of the tensile stress measured from the solidified samples,  $\rho$ : The values of the electrical resistivity measured from the longitudinal section.

IV. CONCLUSION

The principal results of the present work can be summarized as follows;

- a) Experimental observations show that the values of flake spacings ( $\lambda$ ) decreases as growth rate (*V*) increases. The relationships between  $\lambda$  and *V* have been obtained to be  $\lambda = 21.05 V^{-0.43}$ .
- b) *HV* values increase with increasing the values of *V*, but the values of *HV* decrease with increasing the values of  $\lambda$ . The establishment of the relationships among *HV*, *V* and  $\lambda$  can be given as  $HV = 95.36 V^{0.07}$  and  $HV = 31.01 \lambda^{-0.16}$ .
- c) The experimental results show that the values of  $\sigma$  increase with increasing the values of *V* and the values of  $\sigma$  decrease with increasing the values of  $\lambda$ . The establishment of the relationships among  $\sigma$ , *V* and  $\lambda$  can be given as  $\sigma = 59.93 V^{0.16}$  and  $\sigma = 192.81 \lambda^{-0.37}$ .
- d) The values of electrical resistivity ( $\rho$ ) increases with increasing *V* values, but the values of  $\rho$  decrease with increasing the values of  $\lambda$ . The relationships among  $\rho$ , *V* and  $\lambda$  have been obtained to be  $\rho = 9.21 V^{0.05}$  and  $\rho = 3.30 \lambda^{-0.14}$ .
- e) The molten Al-Si-Ni alloy was heated with heating rate of 10 K/min from room temperature to 1200 K. From the trace of heat flow versus temperature, the melting temperature of this ternary alloy was measured to be 856.68 K. The values of the enthalpy of fusion and the specific heat for Al-Si-Ni cast alloy were found to be 209.31 J/g and 0.244 J/(g.K), respectively.

Naukowo-Techniczne.

[2] H. Junga, N. Mangelinck-Noëlb, N. Nguyen-Thib, B. Billiab, "Columnar to Equiaxed Transition During Directional Solidification in Refined AlBased Alloys." Journal of Alloys and Compounds, 484(1-2), 2009, pp. 739-746.

[3] D. Ruvalcaba, R. H. Mathiesen, D. G. Eskin, L. Arnberg, L. Katgerman, "In situ Observations of Dendritic Fragmentation Due to Local Solute Enrichment During Directional Solidification of an Aluminum Alloy." Acta Materialia, 55(13), 2007, pp. 4287-4292.

[4] P. Mikołajczak, L. Ratke, "Directional Solidification of AlSi Alloys with Fe Intermetallic Phases," Archives of Foundry Engineering, 14(1), 2014, pp. 75-78.

[5] P. E. Tomaszewski, "Jan Czochralski - Father of the Czochralski method." Journal of Crystal Growth, 236, 2002, pp. 1-4.

[6] T. Duffar, M. D. Serrano, C. D. Moore, J. Camassel, S. Contreras & B. K. Tanner, "Bridgman Solidification of GaSb in Space." Journal of Crystal Growth, 192, 1998, pp. 63-72.

[7] E. R. Wang, X. D. Hui, S. S. Wang, Y. F. Zhao, G. L. Chen, "Improved Mechanical Properties in Cast Al-Si alloys by Combined Alloying of Fe and Cu." Materials Science and Engineering A, 527, 2010, pp. 78787884.

[8] A. M. Samuel, F. H. Samuel, H. W. Doty, "Observation on the Formation  $\beta$ -Al<sub>5</sub>FeSi Phase in 319 Type Al-Si Alloys." Journal of Materials Science, 31, 1996, pp. 5529-5539.

[9] L. Lu, A.K. Dahle, Mater. Sci. Eng. A, 435-436, 2006, pp. 288-296.

[10] H. Kaya, "Dependency of Electrical Resistivity on the Temperature and Composition of Al-Cu Alloys," Materials Research Innovations, 16 (1), 2012, pp. 224-229,

[11] H. Kaya, E. Çadirli, A. Ülgen, "Investigation of the Effect of Composition on Micro-Hardness and Determination of Thermo-Physical Properties in the Zn-Cu Alloys", Materials & Design, 32, 2011, pp. 900906.

[12] R. Trivedi and W. Kurz, Int. Mat. Rev. 39, 1994, pp.49.

[13] M. I. Yilmazer, H. Kaya, A. Aker, S. Engin, "Influence of the Growth Rate on Physical Properties in the Aluminum-Antimony Eutectic Alloy", International Journal of Materials Engineering and Technology, 9, 2013, pp. 59-76.

- [14] A. Aker, H. Kaya, "Measurements of Microstructural, Mechanical, Electrical and Thermal Properties of an Al-Ni Alloy", *International Journal of Thermo-Physics*, 34 (1), 2013, pp. 267-283.
- [15] M. Smiths, "Measurement of Sheet Resistivities with the Four-Point Probe." (D). *The Bell System Technology*, 37, 1958, pp.711.
- Hardness with Solidification and Microstructure Parameters in the Al Based Alloys." (J). *Applied Surface Science*. 255(5), 2008, pp. 30713078.
- [16] S. Khan, A. Ourdjini, Q. S. Hamed, et al. *Journal Material Science*. 28, 1998, pp. 5957.
- [17] U. Büyük, "Physical and Mechanical Properties of Al-Si-Ni Eutectic Alloy," *Metals and Materials International*, 18, 2012, 6, pp. 933-938.
- [18] H. Kaya, U. Büyük, E. Çadırılı et al. "Measurements of the MicroHardness, Electrical and Thermal Properties of the Al-Ni Eutectic Alloy," *Materials Design*. 34, 2012, pp. 707-712.
- [19] A. Sergeev, V. Mitin, "Electron-Phonon Interaction in Disordered Conductors: Static and Vibrating Scattering Potentials." (J). *Physical Review B*., 61, 2000, pp. 6041-6047.
- [20] Z. Boekelheide, D. W. Cooke, E. Helgren, et al. "Resonant Impurity Scattering and Electron-Phonon Scattering in the Electrical Resistivity of Cr Thin Films." (J). *Physical Review B*, 2009, pp.8013442680134438.